Applying dimension reduction to EEG data by Principal Component Analysis reduces the quality of its subsequent Independent Component decomposition

Fiorenzo Artoni[1,2,*], Arnaud Delorme[3,4,#], Scott Makeig[3,#]

Affiliations

[1]The Biorobotics Institute, Scuola Superiore Sant'Anna, Pisa, Italy

[2]Translational Neural Engineering Laboratory, Center for Neuroprosthetics and Institute of Bioengineering, EPFL – Campus Biotech, Geneve, Switzerland

[3]Swartz Center for Computational Neuroscience, Institute for Neural Computation, University of California San Diego, La Jolla CA 92093-0559

[4]Univ. Grenoble Alpes, CNRS, LNPC UMR 5105, Grenoble, France.

[*] Correspondence to: fiorenzo.artoni@epfl.ch

[#] Equal Contributors

Summary Sentences

- It is currently a common practice to apply dimension reduction to EEG data using PCA before performing ICA decomposition.
- We tested the numbers and quality of meaningful Independent Components (ICs) separated from 72-channel data after different levels of rank reduction to a principal subspace.
- PCA rank reduction (even if removing only 1% of data variance) adversely affected the dipolarity and stability of ICs accounting for potentials arising from brain and known non-brain processes.
- PCA rank reduction also increased uncertainty in the equivalent dipole positions and spectra of the IC brain effective sources across subjects.
- For EEG data at least, PCA rank reduction should therefore be avoided or at least carefully tested on each dataset before applying dimension reduction as a preprocessing step.

Abstract

Independent Component Analysis (ICA) has proven to be an effective data driven method for analyzing EEG data, separating signals from temporally and functionally independent brain and non-brain source processes and thereby increasing their definition. Dimension reduction by Principal Component Analysis (PCA) has often been recommended before ICA decomposition of EEG data, both to minimize the amount of required data and computation time. Here we compared ICA decompositions of fourteen 72-channel single subject EEG data sets obtained (i) after applying preliminary dimension reduction by PCA, (ii) after applying no such dimension reduction, or else (iii) applying PCA only. Reducing the data rank by PCA (even to remove only 1% of data variance) adversely affected both the numbers of dipolar independent components (ICs) and their stability under repeated decomposition. For example, decomposing a principal subspace retaining 95% of original data variance reduced the mean number of recovered 'dipolar' ICs from 30 to 10 per data set and reduced median IC stability from 90% to 76%. PCA rank reduction also decreased the numbers of near-equivalent ICs across subjects. For instance, decomposing a principal subspace retaining 95% of data variance reduced the number of subjects represented in an IC cluster accounting for frontal midline theta activity from 11 to 5. PCA rank reduction also increased uncertainty in the equivalent dipole positions and spectra of the IC brain effective sources. These results suggest that when applying ICA decomposition to EEG data, PCA rank reduction should best be avoided.

Keywords:

Principal component analysis; PCA; Independent component analysis; ICA; electroencephalogram; EEG; Source Localization; Dipolarity; Reliability

I. Introduction

Over the last decade, Independent Component Analysis (ICA) has been steadily gaining popularity among blind source separation (BSS) techniques used to disentangle information linearly mixed into multiple recorded data channels so as to prepare multivariate data sets for more general data mining, in particular for electroencephalographic (EEG) data (Makeig et al., 1996; Makeig et al., 2002). In fact, Local Field activities at frequencies of interest (0.1 Hz to 300 Hz or beyond) arising from near-synchronous activity within a single cortical patch are projected by volume conduction and linearly mixed at scalp EEG channels (Nunez, 1981). A collection of concurrent scalp channel signals may be linearly transformed by ICA decomposition into a new spatial basis of maximally temporally independent component (IC) processes that can be used to assess individual EEG effective source dynamics without prior need for an explicit electrical forward problem head model (Makeig et al., 2004; Onton et al., 2006). Each IC is represented by its pattern of relative projections to the scalp channels (its 'scalp map') and by the time-varying signed strength of its equivalent source signal (Delorme et al., 2012). If electrode locations in the IC scalp maps are known, ICs representing cortical brain processes can typically be localized using either a single equivalent dipole model or a distributed source patch estimate (Acar et al., 2016).

As with most BSS algorithms, obtaining highly reliable extracted components is essential for their correct interpretation and use in further analysis. This is made difficult, however, by noise in the data (from small, irresolvable signal sources, the scalp/sensor interface, or the data acquisition system), by inadequate data sampling (e.g., when not enough data points are available to identify many independent source processes), by algorithmic shortcomings (e.g., convergence issues, response to local minima, etc.) and by inadequate data pre-processing (Artoni et al., 2014; Delorme et al., 2007; Jung et al., 2000). Several classes of stereotyped artifacts (e.g., scalp and neck muscle electromyographic (EMG) activities, electrocardiographic (ECG) signal contamination, single-channel noise produced by occasional disruption in the connections between the electrodes and the scalp, and electro-oculographic (EOG) activity associated with eye blinks, lateral eye movements, and ocular motor tremor) have been found to be well separated from brain activities in EEG data by means of ICA decomposition, provided enough adequately recorded and preprocessed data are available (Jung et al., 2000; Onton and Makeig, 2009).

For such data sets, a second subset of independent components (ICs) have scalp maps that highly resemble the projection of a single equivalent dipole located in the brain (or sometimes the summed projections of two equivalent dipoles, typically located near symmetrically with respect to the interhemispheric fissure). (Delorme et al., 2012) showed that the more mutual information between channel data time courses was reduced by the linear BSS transform the larger number of such 'dipolar'

component processes are present in the resulting ICs. Single equivalent dipole models have scalp maps mathematically *equivalent* to scalp projections of locally coherent (or near-coherent) cortical field activity within single cortical patches whose local spatial coherence also makes them relatively strong effective sources of scalp-recorded EEG signal (Acar et al., 2016; Scherg and Von Cramon, 1986).

Principal Component Analysis (PCA) has been widely used in various research fields (e.g., electromyography, EMG) to reduce the dimensionality of the original sensor space and simplify subsequent analyses. By means of an orthogonal rotation, PCA linearly transforms a set of input data channels into an equal number of linearly-uncorrelated variables (Principal Components, PCs) that each successively account for the largest possible portion of remaining data variance (Kambhatla and Leen, 1997). PCA has been used directly as a BSS method or as a preprocessing step. PCs have been proposed for use in extracting event-related potentials (ERPs) (Bromm and Scharein, 1982), in subsequent frequency domain analyses (Ghandeharion and Erfanian, 2010), or for the identification and removal of artifacts (Casarotto et al., 2004; Ghandeharion and Erfanian, 2010; Lagerlund et al., 1997). In other biomedical fields, PCA has been used, e.g., to increase signal-to-noise ratio (SNR) in evoked neuromagnetic signals (Kobayashi and Kuriki, 1999), and to identify muscle synergies in rectified EMG data, either in combination with Factor Analysis (FA) or to determine the optimal number of muscle synergies to extract, under the assumption that this information is captured by only a few PCs with high variance (Artoni et al., 2013; Ivanenko et al., 2004; Staudenmann et al., 2006). PCA has also been used to discriminate normal and abnormal gait based on vertical ground reaction force time series (Muniz and Nadal, 2009) and to set apart young and adult stair climbing gait patterns (Reid et al., 2010) or age-related kinematic gait parameters (Chester and Wrigley, 2008).

In these and other applications, PCA is used to reduce the dimension of the data. In such applications, the minimum set of largest PCs (i.e., the principal subspace) that accounts for at least some pre-defined variance threshold (usually in the range of 80% to 95% of original data variance) are considered for further analyses. In case of highly correlated data (e.g., 64-128 channel scalp EEG data), as few as 10-15 PCs may account for 95% of data variance. This PC subspace may then be given to an ICA (or similar) algorithm for further transformation with a goal of separating activities arising from different causes and cortical source areas. ICA decomposition minimizes the mutual information between the output component time courses, a stronger criterion than simply eliminating pairwise correlations. Reducing the input space can have the advantage of greatly reducing the computational load in subsequent processing, e.g., the time required for ICA decomposition to converge and the effort required to select which ICs to retain for further analysis (Artoni et al., 2014).

Perhaps for these reasons, most commercial software for EEG analysis advises users to reduce the data dimension using PCA so as to simplify the ICA component selection process and decrease processing time. The possibility of performing PCA during data preprocessing is left as a (non-default) user option in several ICA implementations, e.g. implementations of Infomax ICA (Bell and Sejnowski, 1995; Makeig et al., 1996) and FastICA (Hyvärinen and Oja, 2000), supported by open source EEG analysis environments (Delorme and Makeig, 2004; Oostenveld et al., 2011; Tadel et al., 2011).

For dimensionally redundant datasets, PCA dimension reduction may have a useful place. For example, re-referencing the data to the mean of two scalp channels (e.g., linked earlobes) will reduce the rank of a dataset by one. PCA can be used here to efficiently remove the introduced redundancy, making the data eligible for standard 'complete' (full-rank) ICA decomposition. Else, PCA might be used with very-short recordings to attenuate ICA convergence issues arising from data insufficiency. However, in these cases a viable and possibly preferable alternative is to reduce the number of data channels decomposed.

In a recent comparison of BSS methods applied to EEG data, PCA itself proved to be the least successful of 22 linear ICA/BSS algorithms at extracting physiologically plausible components, and by a considerable margin (Delorme et al., 2012). PCA also performed more poorly at extracting non-brain (artifact) sources from EEG data than infomax ICA (Jung et al., 1998). This is predictable from the objective of PCA, which can be said to be *to 'lump'* as much scalp data variance as possible (from however many underlying sources) into each successive principal component (PC). ICA, on the other hand, tries to *'split'* data variance into component pieces each associated with a single independent component (IC) process. However, the effects of (non-redundant) data dimension reduction by PCA on the quality and reliability of *subsequent* ICA decomposition of the rank-reduced data have not been reported.

If the channel data at hand in fact does represent summed mixtures of a small number of large, temporally independent source activities with near-orthogonal scalp maps, plus a large number of very small ('noise') sources of no particular interest, then performing data rank reduction to the dimension of the large sources using PCA might in some cases improve the signal-to-noise ratio of the large sources and subsequent recovery of the large sources of interest by ICA decomposition. However, when these conditions are not met (e.g., as is typical), when the data are produced by more sources than channels with a continuous range of amplitudes and non-orthogonal scalp projection patterns (scalp maps), then previous research suggests that PCA dimension reduction may adversely affect the quality of the ICA decomposition and, as well, the quality of the ICA-modeled results at subject group level.

Here we report testing this hypothesis by comparing the characteristics of ICA decompositions obtained after applying preliminary rank reduction using PCA (with retained data variances (RVs) of 85%,

95% and 99%) to those obtained by applying ICA or PCA only to the data. We tested the quality of the results in each case by using, as benchmark, the 'dipolarity' of the resulting ICs (a measure of their physiological plausibility) (Delorme et al., 2012), the stability of the ICs across bootstrap replications (Artoni et al., 2014), and group-level robustness of the resulting solutions (source localization, grand average topographies, and frequency spectra).

II. Materials and Methods

The analyses were performed on publicly available EEG data from fourteen subjects (see http://sccn.ucsd.edu/wiki/BSSComparison) acquired during a visual working-memory experiment approved by an Institutional Review board of the University of California San Diego. Further details may be found in (Delorme and Makeig, 2004; Onton et al., 2005). These data were also used by (Delorme et al., 2012) in their study, though as in (Artoni et al., 2014) we here included a data set, originally excluded in (Delorme et al., 2012) because of low data quality. All data and ICA decompositions are made available in (Artoni et al., 2018).

The Experiment. In brief, within each experimental trial the subject stared at a central fixation symbol for 5s (trial start), then a sequence of 3-7 letters were presented for 1.2s each with 200-ms gaps. The letters were colored according to whether they were to be memorized (black) or not (green). After a 2-4 s maintenance period, a probe letter was presented. The subject pressed one of two finger buttons with the dominant hand according to whether (s)he remembered the letter as having been in the memorized letter subset or not. Visual feedback was then provided as to the correctness of the response (a confirmatory beep or cautionary buzz). This also signaled trial end. The 14 subjects (7 males, 7 females, aged 20 – 40 years) each performed 100-150 task trials.

The recorded data used here consisted of 100-150 concatenated 20-24s epochs per subject time locked to letter presentation events, recorded at 250 Hz per channel from 71 scalp channels (69 scalp and 2 periocular electrodes, all referred to the right mastoid) and analog pass band of 0.01 to 100 Hz (SA Instrumentation, San Diego).

Subsequent data preprocessing, performed using MATLAB scripts using EEGLAB (version 14.x) functions (Delorme and Makeig, 2004), comprised (i) high-pass 0.5Hz FIR filtering, (ii) epoch selection ([-700 700] ms time locked to each letter presentation), (iii) whole-epoch mean channel ("baseline") value removal, as this has been reported to give dramatically better ICA decomposition reliability and robustness to spatially non-stereotyped high-amplitude, high-frequency noise (i.e., without a spatially fixed distribution or source, such as produced by unconstrained cap movement) (Groppe et al., 2009).

EEG data variance retained in a principal subspace. Principal component Analysis (PCA) converts observations of correlated variables into a set of linearly uncorrelated orthogonal variables (Principal Components, PCs), ordered in such a way that each PC has the largest possible variance under the constraint of being orthogonal to all preceding components. The first PC is not directionally constrained. Both the time course and the scalp map of smaller PCs are orthogonal to the time courses and maps of all other PCs. Because of this, the scalp maps of later PCs typically resemble checkerboard patterns. PCA can serve both as an exploratory analysis tool and to provide a simplified visualization and interpretation of a multivariate dataset. It has been proposed for use to decompose EEG and ERP data, most often followed by further (orthogonal or non-orthogonal) adjustment (Dien et al., 2007).

Given a $[n, t]$ mean-centered dataset X where n is the number of channels and t the number of time points PCA is computed as the eigenvalue decomposition of the covariance matrix $C_x = XX^T$. The portion of data variance accounted for the first p components, as a percent ratio with respect to the whole dataset variance, is

$$RV_{1:p} = \frac{\sum_{i=1}^{p} \lambda i}{\sum_{i=1}^{n} \lambda i} 100\%$$

where λi is the eigenvalue associated with the i^{th} PC. Retaining a principal subspace of the data (i.e., some number of largest PCs) that makes the retained data, when back-projected into its original channel basis, exceed some specified percentage of the original data variance has been used extensively in different fields to determine the number of PCs (and the concomitant amount of data variance) to retain for further analysis. For instance, dimensionality reduction by PCA has been widely adopted for the extraction of muscle synergies (modeled as PCs) from electromyography (EMG) using a threshold on cumulative retained variance (RV), typically ranging from 75% to 95% of the original (Davis and Vaughan, 1993; Shiavi and Griffin, 1981). The assumption is that small random fluctuations (i.e., noise) can be separated from (relatively large) processes of interest (i.e., task-related information), and removed from the data by discarding small PCs while retaining data variance to the given threshold value. PCA-based variance reduction has also been used as a preprocessing step before applying other blind source separation algorithms, e.g., Factor Analysis, Independent component Analysis (ICA), etc.

The EEG data were here PCA transformed including or not including the two bipolar electro-oculographic (EOG) channels to determine whether this difference would affect the number of PCs needed

to reach a given RV threshold. For each subject, we created two datasets, one including and another not including the two available (vertical and horizontal) electro-oculographic channels, and determined the minimum number of PCs that jointly accounted for least 85%, 95%, 99% of data variance. The first two thresholds are most often used in the literature; the latter we included to test whether even a quite small decrease in RV can produce a difference in the number of *interpretable* EEG independent components extracted from the data.

To test for differences among conditions, we first performed a one-sample Kolmogorov Smirnov test (significance $\alpha = 0.05$) which did not reject the (H0) hypothesis of Gaussianity. We then performed a two-way ANOVA to test for effects of differences in RV threshold (1^{st} level; 85%, 95%, 99%) and type of preprocessing (2^{nd} level; With versus Without EOG), followed by a post-hoc comparison (Tuckey's honest significance difference criterion).

How does PCA affect the capability of ICA to extract interpretable brain and non-brain components? Blind source separation (BSS) methods such as PCA and Independent Component Analysis (ICA), extract an $[m\ n]$ "unmixing matrix" W where n is the number of channels and m the number of independent components (ICs) retained so that

$$S = WX$$

where X is the original $[n, t]$ dataset and S has dimensions $[m, t]$. The i^{th} row of S represents the time course of the i^{th} IC (the IC's 'activation'). The "mixing matrix" A (the pseudoinverse of W, $A = W^{+}$) represents, column-wise, the weights with which the independent component (ICA) projects to the original channels (the IC 'scalp maps'). For sake of simplicity, the terms "IC" will be used below for components of PCA->ICA or ICA-Only origin, PCs for components of PCA-Only origin. Note that the notation for PCA transformation differs from the ICA one, as in PCA-related papers the data X has dimensions $[t, n]$, S_{PCA} $[t, m]$ and W_{PCA} [n, m] and therefore $S_{PCA} = XW_{PCA}$. In this notation, the data channels are represented row-wise to adhere to ICA-related notation and to enhance the readability of the manuscript.

If the electrode locations are available, the columns of A can be represented in interpolated topographical plots of the scalp surface ("scalp maps") that are color-coded according to the relative weights and polarities of the component projections to each of the scalp electrodes. While both decompositions have the same linear decomposition form, PCA extracts components (PCs) with *uncorrelated* time courses and

scalp maps, while ICA extracts *maximally temporally-independent* components (ICs) with unconstrained scalp maps. As linear decompositions, PCA and ICA can be used separately, or PCA can be used as a preprocessing step to ICA to reduce the dimension of the input space and speed ICA convergence.

$$S_{PCA} = W_{PCA}X$$

$$S_{ICA} = W_{ICA}X$$

$$S_{ICAPCA} = W_{ICA}S_{PCA} = W_{ICA}W_{PCA}X = W_{ICAPCA}X$$

Since the scalp maps of most effective brain source ICs strongly resemble the projection of a single equivalent current dipole (Delorme et al., 2012), each component IC_n may be associated with a "dipolarity" value, defined as the percent of its scalp map variance successfully explained by a best-fitting single equivalent dipole model, here computed using a best-fitting spherical four/shell head model (shell conductances: 0.33, 0.0042, 1, 0.33; μS, radii 71, 72, 79, 85) using the DIPFIT functions (version 1.02) within the EEGLAB environment (Delorme and Makeig, 2004; Oostenveld and Oostendorp, 2002):

$$dip(IC_n) = 100\big(1 - resvar(IC_n)\big)\%$$

$resvar(IC_n)$ being the fraction of residual variance explained by the equivalent dipole model,

$$resvar(IC_n) = \frac{var(ScalpMap(IC_n)) - var(DipoleMap(\mathrm{n}))}{var(ScalpMap(IC_n))}$$

For 'quasi-dipolar' components with $dip(IC_n) > 85\%$ and especially for 'near-dipolar' components with $dip(IC_n) > {\sim}95\%$, the position and orientation of their equivalent dipole is likely to mark the estimated location of the component source (with an accuracy depending on the quality of the decomposition and the accuracy of the forward-problem head model used to fit the dipole model). As shown in Figure 3 of (Artoni et al., 2014), ICs with $dip(IC_n) > 85\%$ have the lower likelihood of also having a low quality index (meaning they have stability to resampling). In other words, highly dipolar ICs are more likely to be stable than low dipolar ICs. As in (Delorme et al., 2012) and (Artoni et al., 2014), here we define

"decomposition dipolarity" as the number of ICs with a dipolarity value higher than a given threshold (e.g., 85%, 95%).

To test how preliminary principal PCA subspace selection affects the capability of ICA to extract meaningful artifact and brain components from EEG data, we applied ICA decomposition to each subject's dataset (i) after applying PCA and retaining 85%, 95%, or 99% of the data variance ($PCA_{85}ICA$, $PCA_{95}ICA$, $PCA_{99}ICA$); (ii) by performing ICA decomposition without preliminary PCA (ICA-Only); or (iii) by applying PCA directly with no subsequent ICA (PCA-Only). In each case, we sorted quasi-dipolar ICs (defined here as $dip(IC_n) > 85\%$) into non-brain ("artifact") and "brain" subsets, depending on the location of the model equivalent dipole. The artifact subspace was mainly comprised of recurring, spatial stereotyped (i.e., originating from a spatially fixed source) neck muscle activities or ocular movements. Example results for one subject are shown in Figure 2.

How does PCA preprocessing affect IC dipolarity? After rejecting the null hypothesis of data Gaussianity using a Kolmogorov Smirnov test (significance $\alpha = 0.05$), we statistically compared the number of dipolar ($dip(IC_n) > 85\%$) and quasi-dipolar ($dip(IC_n) > 95\%$)) ICs, produced on average across subjects by PCA-Only, ICA-Only, $PCA_{85}ICA$, $PCA_{95}ICA$, $PCA_{99}ICA$. We used a Kruskal-Wallis test followed by a Tuckey's honest significant difference criterion for post-hoc comparison (Figure 3, left panel).

To avoid limiting the generalizability of the results to dipolarity value thresholds of 85% and 95%, we also compared the number of ICs with dipolarities larger than a range of thresholds ranging from 80% to 99% in 1% increments. In particular, we performed the following comparisons: (i) PCA-Only versus $PCA_{85}ICA$; (ii) $PCA_{85}ICA$ versus $PCA_{95}ICA$; (iii) $PCA_{95}ICA$ versus $PCA_{99}ICA$; (iv) $PCA_{99}ICA$ versus ICA-Only. We used a Wilcoxon signed rank test and reported the p-value for each dipolarity threshold value. A significant p-value at some threshold T implies there were significantly different numbers of ICs with dipolarity above T between conditions (PCA-Only versus $PCA_{85}ICA$; $PCA_{85}ICA$ versus $PCA_{95}ICA$). This test enabled us to determine the exact dipolarity threshold above which the comparisons became non-significant, that is the 'significant dipolarity-difference' point for each comparison (Figure 3, right panel).

We then estimated the probability density function (pdf) for dipolarity values across subjects in PCA-Only, $PCA_{85}ICA$, $PCA_{95}ICA$, $PCA_{99}ICA$ and ICA-Only conditions using kernel density estimation (Bowman and Azzalini, 1997) with a Gaussian kernel, which minimizes the (L2) mean integrated squared error (Silverman, 1986). We then estimated the median and skewness of the distribution (Figure 4).

How does PCA dimension reduction affect component stability? To test the relative stability of ICs obtained after preliminary PCA processing versus ICs obtained by computing ICA directly on the data (ICA-Only), we used RELICA with trial-by-trial bootstrapping (Artoni et al., 2014). RELICA consists of computing W several times from surrogate data sets, formed by randomly selected epochs from the original data set with replacement, always replicating the original data set size.

For each subject, within RELICA we first performed PCA and retained the PCs, in decreasing order of variance, that explained at least 85%, 95%, or 99% variance of the original dataset. Then we applied RELICA using Infomax ICA (Bell and Sejnowski, 1995) in a 'beamICA' implementation (Kothe and Makeig, 2013) after performing 50-fold trial-by-trial bootstrapping (Artoni et al., 2012), drawing points for each trial surrogate at random from the relevant trial with substitution. Infomax directly minimizes mutual information between component time courses (or, equivalently, maximizes the likelihood of the independent component model). Note that ICA is unaffected by the time order of the data points. In the ICA-Only condition, RELICA was applied directly to the original dataset as in (Artoni et al., 2014). RELICA tests the repeatability of ICs appearing in decompositions on bootstrapped versions of the input data to assess the stability of individual ICs to bootstrapping. In RELICA, the sets of ICs returned from each bootstrap decomposition are then clustered according to mutual similarity, σ, defined as the matrix of absolute values of the correlation coefficients between IC time courses, that is $\sigma_{ij} = WR_{ij}W^T$ where R is the covariance matrix of the original data X. The number of clusters was chosen to be equal to the number of PCs back-projected to the scalp channels to create input to the ICA algorithm (or the number of scalp channels in condition ICA-Only). Clusters were identified using an agglomerative hierarchical clustering method, with group average-linkage criterion as agglomeration strategy; see (Artoni et al., 2014) for further details.

We used Curvilinear Component Analysis (CCA), a multidimensional scaling method, to project multivariate points into a two-dimensional space to obtain similarity maps (Himberg et al., 2004). The dispersion of each cluster was measured by the Quality Index (QIc), defined as the difference between the average within-cluster similarities and average between-cluster similarities.

$$QIc = 100 * \left(\frac{1}{|C_m|^2} \sum_{i,j \in C_m} \sigma_{ij} - \frac{1}{|C_m||C_{-m}|} \sum_{i,j \in C_m} \sum_{i,j \in C_{-m}} \sigma_{ij} \right)$$

where C_m is the set of IC indices that belong to the m^{th} cluster, and C_{-m} the set of indices that do not belong, σ_{ij} the similarity between ICs i and j, and $|.|$ indicates the cardinality. The more compact the cluster, the higher the QIc. A perfectly stable, repeatable component has a QIc of 100% (Figure 5).

As with dipolarity values, we estimated the probability density function (pdf) for QIc values over all subjects in the PCA-Only, $PCA_{85}ICA$, $PCA_{95}ICA$, $PCA_{99}ICA$ and ICA-Only conditions and reported both the median and skewness for each. After rejecting the null hypothesis of data Gaussianity using a Kolmogorov Smirnov test (significance $\alpha = 0.05$), we performed a non-parametric one-way analysis of variance (Kruskal-Wallis-Test) on the QIc followed by a Tuckey-Kramer post-hoc comparison to highlight significant difference and reported the ranks.

***How does PCA dimension reduction affect group-level results*?** We tested the effects of PCA preprocessing on the IC clusters, in particular on their spectra and grand-average cluster scalp maps at group level. We examined the left mu (lμ) and frontal midline theta (FMθ) components in the $PCA_{85}ICA$, $PCA_{95}ICA$, $PCA_{99}ICA$ and ICA-Only conditions, as these ICs were of particular relevance to the brain dynamics supporting the task performed by the subjects in the study (Onton et al., 2005). In each condition, ICs for each subject were clustered using IC distance vectors combining differences in equivalent dipole location, scalp projection pattern (scalp map) and power spectral density (1 – 45 Hz) for each IC (Delorme and Makeig, 2004). Given the high dimensionality of the time and frequency features, the dimensionality of the resulting joint vector was reduced to 15 principal components by PCA, which explained 95% of the feature variance (Artoni et al., 2017). Vectors were clustered using a k-means algorithm implemented in EEGLAB, (k = 15). An "outliers" cluster collected components further than three standard deviations from any of the resulting cluster center (Outlier ICs). We checked ICA decompositions and added any seeming appropriate ICs left unclustered by the automated clustering procedure.

For each cluster (lμ and FMθ) and each condition, we then computed (i) the median absolute deviation (MAD) of the distribution of the equivalent dipole positions ($\sigma_x, \sigma_y, \sigma_z$) and (ii) the MAD of the PSD (σ) in the intervals 4 – 8 Hz and 9 - 11 Hz respectively for FMθ and lμ. Figures 7 and 8 also report (i) the single subject scalp topographies pertaining to the cluster; (ii) grand-average scalp topography; (iii) cluster source location within a boundary element model based on the MNI brain template (Montreal Neurological Institute); (iv) median ± MAD of the FMθ and lμ cluster PSDs across subjects (0 – 40 Hz).

III. Results

Results showed that, for all subjects, just 8 ± 2.5 (median ± MAD) PCs were needed to retain 95% of the EEG variance, regardless of whether the EOG data channels were or were not included in the data. Figure 1, panels A,B show a non-linear pattern of explained variance (RV%) with a saturation elbow between 5-10 PCs (85-95% RV%). Above $PCA_{95}ICA$, an increasingly large number of components needed to be added to increase the RV%.

FIGURE 1 ABOUT HERE

Extraction of brain and non-brain (artifact) components. Figure 2 shows, for a representative subject, the scalp topographies of quasi-dipolar components (dipolarity > 85%), those extracted directly with PCA (PCA-only), directly by ICA (Infomax) without PCA, or by ICA after retaining the minimum number of PCs that explained 85% ($PCA_{85}ICA$), 95% ($PCA_{95}ICA$) and 99% ($PCA_{99}ICA$) of dataset variance respectively. The quasi-dipolar ICs were then separated into 'brain ICs' (i.e., having a brain origin) and 'artifact (non-brain) ICs' mainly accounting for scalp/neck muscle and ocular movement artifact. For this subject only 3 components (PCs) extracted by PCA-only reached the 85% dipolarity threshold. Separate vertical and lateral eye movement ICs were extracted in the $PCA_{85}ICA$, $PCA_{95}ICA$ and $PCA_{99}ICA$, and ICA-Only conditions, but not in the PCA-Only condition. Left and right neck muscle components, as well as the left mu components were not extracted in either the $PCA_{85}ICA$ or PCA-Only conditions, and the higher the level of explained variance (RV) the less widespread the scalp maps (e.g., for those accounting for lateral eye movements). The number of artifact ICs as well as the number of brain ICs increased with the amount of variance retained (respectively, 3 non-brain, artifact and 3 brain ICs in RV85, 5 artifact and 5 brain ICs in $PCA_{95}ICA$, 7 artifact and 12 brain ICs in $PCA_{99}ICA$, and 12 artifact and 15 brain ICs in ICA-Only).

FIGURE 2 ABOUT HERE

Independent component dipolarity. Over the whole subject pool, the left top (A) and bottom (B) panels of Figure 3 show the box plot of the across-subjects median numbers of extracted quasi-dipolar ($dip(IC)$>85%, top left panel A) and near-dipolar ($dip(IC)$>95%, bottom left panel B) ICs. Statistical

comparisons showed that the ICA-Only processing pipeline produced a significantly higher number of quasi-dipolar and near-dipolar components than the pipelines PCA-Only, $PCA_{85}ICA$, $PCA_{95}ICA$ ($p<0.001$), and even $PCA_{99}ICA$ ($p<0.01$ for DIP ≥ 85%, $p<0.05$ for DIP ≥ 95%). The number of quasi- and near-dipolar ICs in $PCA_{99}ICA$ was also significantly higher than in $PCA_{95}ICA$, $PCA_{85}ICA$, and PCA-Only ($p<0.0001$ for DIP ≥ 85%, $p<0.001$ for DIP ≥ 95%). No significant differences were found between the numbers of near-dipolar ICs in the PCA-Only, $PCA_{85}ICA$ and $PCA_{95}ICA$ conditions. The dotted red lines in Figure 3 (A and B) highlight a positive trend in the number of quasi-dipolar components, including a change of slope in conditions $PCA_{95}ICA$ and $PCA_{99}ICA$, as successive PCs are increasingly smaller themselves.

The right panels of Figure 3C show the estimated probabilities of significant difference in the number of dipolar ICs for several pairwise condition contrasts for threshold values ranging from DIP > 80% to DIP > 99% (x axis). In the contrast between PCA-Only and $PCA_{85}ICA$ conditions, the significant condition difference threshold ($p<0.05$) is never reached (top right panel). For other comparisons in which ICA is used, significant condition differences appear for all but the following dipolarity threshold values: DIP ≥ 95% ($PCA_{85}ICA$ versus $PCA_{95}ICA$, second right panel) and DIP ≥ 97% ($PCA_{95}ICA$ versus $PCA_{99}ICA$, third right panel; $PCA_{99}ICA$ versus ICA-Only, bottom right panel). Panel D shows for each subject the number of dipolar ICs (at thresholds DIP > 85%, left panel; DIP > 95%, right panel) against the number of total ICs retained after applying PCA with $PCA_{85}ICA$ (black dots), $PCA_{95}ICA$ (green dots), $PCA_{99}ICA$ (blue dots) and ICA only (red dots) respectively. For each subject, relative dots are connected by a dashed blue line. The red dotted line delimits the region where the number of dipolar ICs is equal to the number of ICs. The number of dipolar ICs increases monotonically and nonlinearly with the #ICs available. The sheaf of lines is adherent to the delimitation line for #ICs < 20 and DIP>85% and for #ICs < 10 for DIP > 95%.

FIGURE 3 ABOUT HERE

Figure 4 shows the distribution of dipolarities across all subject datasets. The skewness of the distributions is negative (sk = -2.1 for $PCA_{85}ICA$, -1.5 for $PCA_{95}ICA$, -0.8 for $PCA_{99}ICA$ and ICA-Only) for all conditions involving ICA decomposition (i.e., except in PCA-Only, sk = +2.1). The median dipolarity values for PCA→ICA pipelines range from 80% (ICA-Only and RV99%) to over 90% ($PCA_{85}ICA$), whereas for PCA-Only, the median component dipolarity is near 12% (profoundly non-dipolar).

FIGURE 4 ABOUT HERE

Independent component stability. Figure 5 shows, for a representative subject, the dispersion of left hand-area (strong mu rhythm), central posterior (strong alpha activity), and eye blink artifact clusters in the two-dimensional CCA space computed by RELICA for four ICA-involved conditions. Note that the corresponding cluster quality (QIc) values for the visualized ICA-Only ICs (95%, 99%, and 98%) are higher than for corresponding ICs from the $PCA_{85}ICA$ (NA, 83%, 88%), $PCA_{95}ICA$ (83%, 81%, 89%) and $PCA_{99}ICA$ (78%, 85%, 89%) pipelines.

FIGURE 5 ABOUT HERE

This was confirmed by assessing the QIc distributions across subjects (Figure 6). The QIc distribution for ICA-Only is centered towards higher QIc values than for the other conditions as measured by the skewness (-0.3, -0.8, -0.6, and -1.9 for $PCA_{85}ICA$, $PCA_{95}ICA$, $PCA_{99}ICA$ and ICA-Only respectively). Figure 6 (bottom panel) shows that the median QIc in the ICA-Only condition was significantly higher ($p<0.001$) than for other conditions, while no significant difference appeared between the three PCA→ICA conditions. In other words, applying PCA dimension reduction during preprocessing, even while retaining 99% of dataset variance, decreased the stability of the returned ICs.

FIGURE 6 ABOUT HERE

Group-level results. To determine the effects of PCA preprocessing on group-level results we analyzed IC clusters exhibiting clear left-hemisphere (right-hand) area (9-11 Hz) mu rhythm ($l\mu$) and frontal midline (4-8 Hz) theta band ($fM\theta$) activities, respectively. Figure 7 shows the results of IC effective source clustering at the group level plus grand-average power spectral density for cluster $fM\theta$. While 11 of 14 subjects exhibited a clear frontal midline theta component activation in the ICA-Only condition decompositions, the number of $fM\theta$ cluster ICs decreased to just 6 in $PCA_{99}ICA$, to 5 in $PCA_{95}ICA$, and to 4 in $PCA_{85}ICA$. This means that for 5 of the subjects (11-6=5), $fM\theta$ ICs could be found only when the last 1% of explained variance was included in the ICA decomposition, and for two more subjects only when at least the next 4%

(altogether, 95%) of data variance was retained (Figure 7, 1st column). The new fMθ ICs recovered by the $PCA_{95}ICA$ and $PCA_{99}ICA$ decompositions were not themselves small. For example, a lμ IC that appeared in the $PCA_{99}ICA$ decomposition, but not in the $PCA_{95}ICA$ for one subject accounted for over 6% of data variance – more than the additional amount of data variance retained in $PCA_{99}ICA$ versus $PCA_{95}ICA$.

While the grand-average cluster scalp maps (except in $PCA_{85}ICA$) appear similar to one another, the $PCA_{99}ICA$ condition cluster only includes contributions from half the subject population (versus 11 of 14 for ICA-Only). The cluster IC equivalent dipole locations for the fMθ cluster also had a higher median absolute deviation (MAD) in $PCA_{99}ICA$ ($\sigma_x = 4.5, \sigma_y = 15.1, \sigma_z = 20.1$), $PCA_{95}ICA$ ($\sigma_x = 7.3, \sigma_y = 27.9, \sigma_z = 20.0$) and $PCA_{85}ICA$ ($\sigma_x = 5.2, \sigma_y = 25.7, \sigma_z = 25.0$) than in the ICA-Only condition ($\sigma_x = 2.6, \sigma_y = 10.5, \sigma_z = 8.3$), indicating higher scattering of equivalent dipole effective source locations across subjects when PCA dimension reduction was used (Figure 7, 3rd column). As well, the θ peak in the cluster mean PSD (Figure 7, 4th column) is sharper, and the PSD MAD lower, in the ICA-Only condition ($\sigma = 0.7$) than in the PCA→ICA conditions: $PCA_{99}ICA$, $\sigma = 0.9$; $PCA_{95}ICA$, $\sigma = 1.2$; $PCA_{85}ICA$, $\sigma = 3.2$.

FIGURE 7 ABOUT HERE

Similar conclusions can be drawn for the left hand (right hemisphere) area mu (lμ) cluster. Figure 8 shows that the lμ cluster represents effective source activities from 8, 7, 6 and no subjects in the ICA-Only, $PCA_{99}ICA$ $PCA_{95}ICA$ and $PCA_{85}ICA$ conditions, respectively (no lμ cluster was found in the $PCA_{85}ICA$ ICs). The lμ cluster equivalent dipole MAD is ($\sigma_x = 5.7, \sigma_y = 11.0, \sigma_z = 7.6$) in ICA-Only, ($\sigma_x = 7.4, \sigma_y = 8.8, \sigma_z = 7.9$) in $PCA_{99}ICA$, and ($\sigma_x = 11.7, \sigma_y = 11.0, \sigma_z = 14.4$) in $PCA_{95}ICA$. Regarding the PSD, the beta band peak in the PSD (18-24 Hz range) can only be seen clearly in results from ICA-Only. The MAD of the PSD also increases as ICA is applied to smaller principal subspaces of the data: $\sigma = 1.7$ for ICA-Only; $\sigma = 2.5$ for $PCA_{99}ICA$; $\sigma = 2.6$ for $PCA_{95}ICA$.

FIGURE 8 ABOUT HERE

IV. Discussion

PCA-based rank reduction affects the capability of ICA to extract dipolar brain and non-brain (artifact) components. Figure 1 shows a nonlinear relationship between cumulative retained variance and the number of PCs retained. Here a ten-dimension principal subspace (the first 10 PCs) comprised as much as 95% of the ~70-channel dataset variance. To increase the variance retained by another 4%, 15 more (smaller) PCs were required, and 15 more (smaller still) were needed to reach 99%. The first (largest) PCs were likely dominated by large ocular and other non-brain artifacts, as there were no significant differences in cumulative variance retained depending on whether EOG channels were included in or excluded.

The aim of principal component analysis is to extract both spatially and temporally orthogonal components, each in turn maximizing the amount of additional variance they contribute to the accumulating principal subspace. This process can be characterized as "lumping" together portions of the activities of many temporally independent, physiologically and functionally distinct, but spatially non-orthogonal effective IC sources. Fulfilling this objective means that, typically, low-order principal components are dominated by large, typically non-brain artifact sources such as eye blinks (Möcks and Verleger, 1986), while high-order principal component scalp maps resemble checkerboards of various densities.

Figure 4 shows the pooled dipolarity distribution of ICs and PCs across the subjects. For PCs, this distribution is centered on low values (near 10%, highly incompatible with a single source equivalent dipole) and has high positive skewness (2.1). ICA, by maximizing signal independence and removing the orthogonality constraint on the component scalp maps, also produces many ICs with high scalp map dipolarity, producing a dipolarity distribution with high median (about 90%) and negative skewness. This result is in accord with (Delorme et al., 2012) who discovered a positive linear correlation, for some 18 linear decomposition approaches, between the amount of mutual information reduction (between time courses) produced in linearly transforming the data from a scalp channel basis to a component basis, and the number of near-dipolar components extracted.

As a further confirmation of this, here only three dipolar PCs on average could be extracted from each subject by PCA-Only (Figures 2 and 3). The scalp map of the first PC resembles the scalp projection of lateral eye movement artifact; the second PC appears to combine scalp projections associated with vertical eye movement artifact (e.g., IC1 in $PCA_{85}ICA$), alpha band activity (IC1, $PCA_{95}ICA$) and neck muscle artifact (neck muscle IC7, $PCA_{99}ICA$).

Any full-rank, well-conditioned preliminary linear transformation of the data (e.g., PCA with 100% variance retained) does not affect ICA results. Also, variance alone is insufficient for separating physiologically meaningful components and noise (Kayser and Tenke, 2006). As it is, by reducing the rank of the data by PCA before applying ICA also reduced the number of brain and non-brain artifact dipolar ICs that were extracted. Figure 2 shows that ICs accounting for vertical and lateral eye movement artifacts (blue dashed box) were always extracted. However, for the lateral eye movement component, the higher the retained variance, the less affected the channels other than the frontal ones.

Figure 3 (panels A, B) shows the median numbers of quasi-dipolar (DIP ≥ 85%) and near-dipolar (DIP ≥ 95%) ICs, respectively, that were extracted depending on the amount of retained variance. Statistical analysis showed a significant increase ($p<0.01$ for DIP ≥ 85%, $p<0.05$ for DIP ≥ 95%) in the numbers of dipolar components produced by ICA-Only in comparison to $PCA_{99}ICA$. The number of retained PCs affects the number of dipolar ICs that ICA can extract subsequently. Using a stricter near-dipolar threshold (DIP ≥ 95%), the increasing numbers of dipolar ICs returned on average by $PCA_{95}ICA$, $PCA_{99}ICA$, and ICA-Only for the 14 subjects were 4, 6, and 9 respectively. Using the looser quasi-dipolar threshold (DIP ≥ 85%), the larger numbers of ICs rated as dipolar (8, 23, 31) were less dramatically affected by dimension reduction (Figure 3). Condition-to-condition differences in numbers of returned 'dipolar' components (Figure 3C) were statistically significant for all but the strictest dipolarity thresholds (reached by relatively few ICs in any condition).

The paucity of near-dipolar ICs likely in part arises from disparities between the common MNI template electrical head model used here to compute dipolarity values and more accurate individualized head models (e.g. built from subject MR head images). In Fig. 3C, $PCA_{85}ICA$ never produces significantly more dipolar ICs than PCA-Only; evidently, retaining only 85% of explained variance (e.g., within the first 10 PCs) left too few degrees of freedom for the ICA algorithm to be able to extract a significantly higher number of dipolar ICs than PCA alone.

In other words, the extra degrees of freedom allowed by higher retained variances (ideally 100%, i.e., without applying PCA dimension reduction at all), allows ICA to re-distribute data variance to achieve stronger MI reduction, thereby separating more component processes compatible with spatially coherent activity across a single cortical patch. The significant differences, at all dipolarity threshold values lower than DIP>97%, in the numbers of dipolar components in $PCA_{99}ICA$ versus ICA-Only, shows the importance for ICA effectiveness of keeping the whole data intact rather than reducing it, even slightly, to a principal subspace.

The caution raised by these results concerning PCA dimension reduction prior to ICA decomposition of EEG data raises questions concerning other types of biological time series data to which ICA can be usefully applied, for example fMRI (McKeown et al., 1997), MEG (Iversen and Makeig, 2014; Vigário et al., 1998), ECoG (Whitmer et al., 2010) . Experience suggests to us that the same may be true for data reduction by (low-pass) frequency band filtering, although here we find that removing (often large) low-frequency activity below ~1 Hz before ICA decomposition may improve, rather than degrade, success in returning dipolar ICs. This might reflect the differing origins and possible spatial non-stationary of low-frequency EEG processes, an assumption that needs more detailed testing. Based on experience and consistent with the results reported in (Winkler et al., 2015) we would recommend applying ICA on ~1-Hz high-passed data and, if different preprocessing steps are required (e.g., different high-pass filtering cutoff frequencies, different artifact removal pipelines), consider re-applying the model weights to the unfiltered raw data (e.g., to remove blinks from low-frequency activity)(Artoni et al., 2017). However, note that in this case one may not assume that the low-frequency portions of the signals have necessarily been correctly decomposed into their functionally distinct source processes, since some other low-frequency only processes may contribute to the data. It is also important to note that avoiding PCA as a preprocessing step does not guarantee a high-quality ICA decomposition, as quality is also affected also by other factors including inadequate data sampling (e.g., number of channels and/or effective data points available), inadequate data pre-processing, algorithm deficiencies and noise (Artoni et al., 2014). One of the reasons behind the application of PCA rank reduction by many users before ICA decomposition is likely the easier interpretation of a lower number of components. However, fixing the PCA variance threshold introduces variability in the number components available for each dataset and vice versa fixing the rank results in explained variance variability across datasets. A number of methods, that of Winkler et al. for one (Winkler et al., 2011), are available to aid in IC selection or classification.

For EEG data, valuable information about component process independence is contained in the final 1% of data variance (projected from the smallest PCs), and reducing the rank of the data so as to retain even as much as 99% of its variance impairs the capability of ICA to extract meaningful dipolar brain and artifact components. A principal reason for this is that PCA rank reduction increases the EEG overcompleteness problem of there being more independent EEG effective sources than degrees of freedom available to separate them. The objective of PCA to include as much data variance as possible in each successive PC, combined with the influence this entails on PCs to have mutually orthogonal scalp maps, means that PCs almost never align with a single effective source (unless one source is much larger than all others and so dominates the first PC). That is, typically some portions of the activities of many the independent effective

sources are summed in every PC. Choosing a PC subset reduces the number of degrees of freedom available to ICA while typically *not* reducing the number of effective brain and non-brain sources contributing to the channel data. Because principal component scalp maps must also be mutually orthogonal, scalp maps of successively smaller PCs typically have higher and higher spatial frequencies (and 'checkerboard' patterns). While PCA rank reduction might not degrade highly stereotyped components such as eye blinks, not removing small (high spatial-frequency) PCs from the data allows ICA to return dipolar IC scalp maps whose spatial frequency profiles, dominated by low (broad) spatial frequencies typical of dipolar source projections, conform more precisely to the true scalp projection patterns of the independent cortical and non-brain effective source processes.

PCA-based rank reduction decreased IC reliability across subjects. Measures of IC dipolarity and stability to data resampling are both important to assessment of *within*-subject IC reliability. While IC dipolarity provides a measure of physiological plausibility (Delorme et al., 2012), IC stability measures robustness to small changes in the data selected for decomposition (Artoni et al., 2014). Assessing IC reliability (dipolarity and stability) at the single-subject level is important to avoid mistakenly entering unreliable or physiologically uninterpretable ICs into group-level analyses.

Figure 5 shows the two-dimensional CCA cluster distributions and exemplar IC scalp maps for three IC clusters accounting for left mu, central alpha, and eye blink artifact activities respectively. As shown there, for ICA-Only the cluster quality indices for the three example clusters are in the 95-99% range, while for the three PCA→ICA conditions the equivalent component cluster quality indices range from only 78% to 89%, meaning that the IC time courses within bootstrap repetitions of the ICA decomposition (represented by dots in the Fig. 5 CCA plane plots) are less distinctly more correlated within-cluster versus between-clusters. The IC clusters appear more crisply defined in the CCA plane for ICA-Only (though note its larger data rank and, therefore, larger number of ICs). Figure 6 shows that across subjects, brain source ICs had a higher quality index QIc in the ICA-Only condition, for which the distribution was strongly skewed toward high QIc (skewness, -1.9; median QIc, 90%, significantly higher [$p<0.001$] than for the three PCA→ICA conditions). The QIc indirectly indexes the variability of the ICA decomposition by measuring the dispersion of an IC cluster within the 2-D CCA measure space (Artoni et al., 2014). Sources of variability in the ICA decomposition are noise, algorithm convergence issues (e.g., local minima), non-stationary artifacts etc. Applying PCA dimension reduction with a specific RV% threshold, makes ICA operate on a somewhat different data sample in each bootstrap repetition, thus likely introducing a further source of variability and further decreasing the QIc.

PCA-based rank reduction degraded the group-level results. The quality of information provided by group-level results depends on the reliability (dipolarity and stability) of the individual ICs, as supported by the results shown in Figures 7 and 8. For the frontal midline theta cluster (Figure 7), the lower the PCA-retained variance, the fewer the subjects represented in the cluster (e.g., 11 of 14 for ICA-Only versus 4 of 14 for $PCA_{85}ICA$). For the mu cluster, in $PCA_{85}ICA$ no ICs reached the DIP > 85% threshold. Lack of uniform group representation is a distinct complication for performing group statistical comparisons on ICA-derived results, as modern statistical methods taking into account missing data should then be used (Dempster et al., 1977; Hamer and Simpson, 2009; Sinharay et al., 2001).

Cluster mean scalp maps (Fig. 7, 2nd column,) are also affected by the lower IC representation. The blue color of the average scalp map ($PCA_{85}ICA$) over the occipital area is symptom of spurious brain activity captured by the cluster, other than the frontal midline theta (Onton et al., 2005). This is confirmed by source localization (Figures 7 and 8, 3rd column): equivalent dipoles are more scattered with $PCA_{85}ICA$ (only frontal midline theta), $PCA_{95}ICA$ than with $PCA_{99}ICA$ and ICA-Only. The lower the variance retained, the higher the standard errors, $\sigma_x, \sigma_y, \sigma_z$. While this might be ascribed to the lack of representation of the cluster by a sufficient number of ICs for $PCA_{85}ICA$, the higher size of the cluster with lower RV% seems to confirm that ICs are not as well localized as with, e.g., ICA-Only, which suggests a relation between the total number of dipolar and reliable ICs obtained over all subjects and the source localization variability for group-level clusters. Source localization variability depends on many factors, e.g., inter-subject variability arising from different cortical convolutions across subjects, unavailability of MRI scans and electrode co-registration, source localization algorithm deficiencies, etc. However, preliminary rank reduction by PCA can further increase source position variability and impair the possibility to draw conclusions at group level.

Rank reduction also impacts task-based measures such as power spectral densities (PSDs). The variability across subjects in the theta band across subjects (Figure 7, 4th column) is maximum for $PCA_{85}ICA$ and minimum for ICA-Only (which here also produced a visually more pronounced theta peak). The same is true for the mu IC (Figure 8, 4th column): the typical 18-20 Hz second peak is clearly visible in the ICA-Only results, while it is barely hinted for $PCA_{99}ICA$ and does not appear for $PCA_{95}ICA$. This result shows that rank reduction can have unpredictable effects not only on source localization and reliability of ICs but also on dynamic source measures such as PSD.

Conclusion. These results demonstrate that reducing the data rank to a principal subspace using PCA, even to remove as little as 1% of the original data variance, can adversely affect both the dipolarity and stability of independent components (ICs) extracted thereafter from high-density (here, 72-channel) EEG data, as

well as degrading the overall capability of ICA to separate functionally identifiable brain and non-brain (artifact) source activities at both the single subject and group levels. These conclusions might vary slightly depending on the amount of data available (its length and number of channels), preprocessing pipeline, type of subject task, etc. Further work will focus on testing the extensibility of these findings to low-density (e.g., 16-32 channel), ultra-high-density (128+ channel), brief (too few 10 minutes) and lengthy (e.g., several hour) recordings. However, it is possible to conclude that contrary to common practice in this and related research fields, PCA-based dimension reduction of EEG data should be avoided or at least carefully considered and tested on each dataset before applying it during preprocessing for ICA decomposition.

Funding and Acknowledgments

Dr. Artoni's contributions were supported by the European Union's Horizon 2020 research and innovation programme under Marie Skłodowska Curie grant agreement No. 750947 (project BIREHAB). Drs. Makeig and Delorme's contributions were supported by a grant (R01 NS047293) from the U.S. National Institutes of Health (NIH) and by a gift to the Swartz Center, UCSD from The Swartz Foundation (Old Field NY). We acknowledge Dr. Makoto Miyakoshi for his support and helpful discussions.

References

Acar, Z.A., Acar, C.E., Makeig, S., 2016. Simultaneous head tissue conductivity and EEG source location estimation. Neuroimage 124, 168-180.

Artoni, F., Delorme, A., Makeig, S., 2018. A visual working memory dataset collection with bootstrap Independent Component Analysis for comparison of electroencephalogram preprocessing pipelines. Data In Brief Submitted.

Artoni, F., Fanciullacci, C., Bertolucci, F., Panarese, A., Makeig, S., Micera, S., Chisari, C., 2017. Unidirectional brain to muscle connectivity reveals motor cortex control of leg muscles during stereotyped walking. Neuroimage 159, 403-416.

Artoni, F., Gemignani, A., Sebastiani, L., Bedini, R., Landi, A., Menicucci, D., 2012. ErpICASSO: a tool for reliability estimates of independent components in EEG event-related analysis. Conf Proc IEEE Eng Med Biol Soc 2012, 368-371.

Artoni, F., Menicucci, D., Delorme, A., Makeig, S., Micera, S., 2014. RELICA: a method for estimating the reliability of independent components. Neuroimage 103, 391-400.

Artoni, F., Monaco, V., Micera, S., 2013. Selecting the best number of synergies in gait: preliminary results on young and elderly people. IEEE Int Conf Rehabil Robot 2013, 6650416.

Bell, A.J., Sejnowski, T.J., 1995. An information-maximization approach to blind separation and blind deconvolution. Neural Comput 7, 1129-1159.

Bowman, A.W., Azzalini, A., 1997. Applied smoothing techniques for data analysis: the kernel approach with S-Plus illustrations. OUP Oxford.

Bromm, B., Scharein, E., 1982. Principal component analysis of pain-related cerebral potentials to mechanical and electrical stimulation in man. Electroencephalography and clinical neurophysiology 53, 94-103.

Casarotto, S., Bianchi, A.M., Cerutti, S., Chiarenza, G.A., 2004. Principal component analysis for reduction of ocular artefacts in event-related potentials of normal and dyslexic children. Clinical neurophysiology 115, 609-619.

Chester, V.L., Wrigley, A.T., 2008. The identification of age-related differences in kinetic gait parameters using principal component analysis. Clinical Biomechanics 23, 212-220.

Davis, B.L., Vaughan, C.L., 1993. Phasic behavior of EMG signals during gait: use of multivariate statistics. Journal of Electromyography and Kinesiology 3, 51-60.

Delorme, A., Makeig, S., 2004. EEGLAB: an open source toolbox for analysis of single-trial EEG dynamics including independent component analysis. J Neurosci Methods 134, 9-21.

Delorme, A., Palmer, J., Onton, J., Oostenveld, R., Makeig, S., 2012. Independent EEG sources are dipolar. PLoS One 7, e30135.

Delorme, A., Sejnowski, T., Makeig, S., 2007. Enhanced detection of artifacts in EEG data using higher-order statistics and independent component analysis. Neuroimage 34, 1443-1449.

Dempster, A.P., Laird, N.M., Rubin, D.B., 1977. Maximum likelihood from incomplete data via the EM algorithm. Journal of the royal statistical society. Series B (methodological), 1-38.

Dien, J., Khoe, W., Mangun, G.R., 2007. Evaluation of PCA and ICA of simulated ERPs: Promax vs. Infomax rotations. Human brain mapping 28, 742-763.

Ghandeharion, H., Erfanian, A., 2010. A fully automatic ocular artifact suppression from EEG data using higher order statistics: Improved performance by wavelet analysis. Medical engineering & physics 32, 720-729.

Groppe, D.M., Makeig, S., Kutas, M., 2009. Identifying reliable independent components via split-half comparisons. Neuroimage 45, 1199-1211.

Hamer, R.M., Simpson, P.M., 2009. Last observation carried forward versus mixed models in the analysis of psychiatric clinical trials. Am Psychiatric Assoc.

Himberg, J., Hyvärinen, A., Esposito, F., 2004. Validating the independent components of neuroimaging time series via clustering and visualization. Neuroimage 22, 1214-1222.

Hyvärinen, A., Oja, E., 2000. Independent component analysis: algorithms and applications. Neural networks 13, 411-430.

Ivanenko, Y.P., Poppele, R.E., Lacquaniti, F., 2004. Five basic muscle activation patterns account for muscle activity during human locomotion. The Journal of physiology 556, 267-282.

Iversen, J.R., Makeig, S., 2014. MEG/EEG data analysis using EEGLAB. Magnetoencephalography. Springer, pp. 199-212.

Jung, T.-P., Humphries, C., Lee, T.-W., Makeig, S., McKeown, M.J., Iragui, V., Sejnowski, T.J., 1998. Removing electroencephalographic artifacts: comparison between ICA and PCA. Neural Networks for Signal Processing VIII, 1998. Proceedings of the 1998 IEEE Signal Processing Society Workshop. IEEE, pp. 63-72.

Jung, T.-P., Makeig, S., Humphries, C., Lee, T.-W., Mckeown, M.J., Iragui, V., Sejnowski, T.J., 2000. Removing electroencephalographic artifacts by blind source separation. Psychophysiology 37, 163-178.

Kambhatla, N., Leen, T.K., 1997. Dimension reduction by local principal component analysis. Neural computation 9, 1493-1516.

Kayser, J., Tenke, C.E., 2006. Consensus on PCA for ERP data, and sensibility of unrestricted solutions. Clinical neurophysiology 117, 703-707.

Kobayashi, T., Kuriki, S., 1999. Principal component elimination method for the improvement of S/N in evoked neuromagnetic field measurements. IEEE Transactions on Biomedical Engineering 46, 951-958.

Kothe, C.A., Makeig, S., 2013. BCILAB: a platform for brain–computer interface development. Journal of neural engineering 10, 056014.

Lagerlund, T.D., Sharbrough, F.W., Busacker, N.E., 1997. Spatial filtering of multichannel electroencephalographic recordings through principal component analysis by singular value decomposition. Journal of clinical neurophysiology 14, 73-82.

Makeig, S., Bell, A.J., Jung, T.-P., Sejnowski, T.J., 1996. Independent component analysis of electroencephalographic data. Advances in neural information processing systems, pp. 145-151.

Makeig, S., Debener, S., Onton, J., Delorme, A., 2004. Mining event-related brain dynamics. Trends in cognitive sciences 8, 204-210.

Makeig, S., Westerfield, M., Jung, T.-P., Enghoff, S., Townsend, J., Courchesne, E., Sejnowski, T.J., 2002. Dynamic brain sources of visual evoked responses. Science 295, 690-694.

McKeown, M.J., Makeig, S., Brown, G.G., Jung, T.-P., Kindermann, S.S., Bell, A.J., Sejnowski, T.J., 1997. Analysis of fMRI data by blind separation into independent spatial components. Naval Health Research Center, San Diego, CA.

Möcks, J., Verleger, R., 1986. Principal component analysis of event-related potentials: a note on misallocation of variance. Electroencephalography and Clinical Neurophysiology/Evoked Potentials Section 65, 393-398.

Muniz, A., Nadal, J., 2009. Application of principal component analysis in vertical ground reaction force to discriminate normal and abnormal gait. Gait & posture 29, 31-35.

Nunez, P.L., 1981. A study of origins of the time dependencies of scalp EEG: I-theoretical basis. IEEE Transactions on Biomedical Engineering, 271-280.

Onton, J., Delorme, A., Makeig, S., 2005. Frontal midline EEG dynamics during working memory. Neuroimage 27, 341-356.

Onton, J., Makeig, S., 2009. High-frequency broadband modulations of electroencephalographic spectra. Frontiers in human neuroscience 3.

Onton, J., Westerfield, M., Townsend, J., Makeig, S., 2006. Imaging human EEG dynamics using independent component analysis. Neuroscience & Biobehavioral Reviews 30, 808-822.

Oostenveld, R., Fries, P., Maris, E., Schoffelen, J.-M., 2011. FieldTrip: open source software for advanced analysis of MEG, EEG, and invasive electrophysiological data. Computational intelligence and neuroscience 2011, 1.

Oostenveld, R., Oostendorp, T.F., 2002. Validating the boundary element method for forward and inverse EEG computations in the presence of a hole in the skull. Human brain mapping 17, 179-192.

Reid, S.M., Graham, R.B., Costigan, P.A., 2010. Differentiation of young and older adult stair climbing gait using principal component analysis. Gait & posture 31, 197-203.

Scherg, M., Von Cramon, D., 1986. Evoked dipole source potentials of the human auditory cortex. Electroencephalography and Clinical Neurophysiology/Evoked Potentials Section 65, 344-360.

Shiavi, R., Griffin, P., 1981. Representing and clustering electromyographic gait patterns with multivariate techniques. Medical and Biological Engineering and Computing 19, 605-611.

Silverman, B.W., 1986. Density estimation for statistics and data analysis. CRC press.

Sinharay, S., Stern, H.S., Russell, D., 2001. The use of multiple imputation for the analysis of missing data. Psychological methods 6, 317.

Staudenmann, D., Kingma, I., Daffertshofer, A., Stegeman, D.F., van Dieën, J.H., 2006. Improving EMG-based muscle force estimation by using a high-density EMG grid and principal component analysis. IEEE Transactions on Biomedical Engineering 53, 712-719.

Tadel, F., Baillet, S., Mosher, J.C., Pantazis, D., Leahy, R.M., 2011. Brainstorm: a user-friendly application for MEG/EEG analysis. Computational intelligence and neuroscience 2011, 8.

Vigário, R., Särelä, J., Oja, E., 1998. Independent component analysis in wave decomposition of auditory evoked fields. ICANN 98. Springer, pp. 287-292.

Whitmer, D., Worrell, G., Stead, M., Lee, I.K., Makeig, S., 2010. Utility of independent component analysis for interpretation of intracranial EEG. Frontiers in human neuroscience 4.

Winkler, I., Debener, S., Müller, K.-R., Tangermann, M., 2015. On the influence of high-pass filtering on ICA-based artifact reduction in EEG-ERP. Engineering in Medicine and Biology Society (EMBC), 2015 37th Annual International Conference of the IEEE. IEEE, pp. 4101-4105.

Winkler, I., Haufe, S., Tangermann, M., 2011. Automatic classification of artifactual ICA-components for artifact removal in EEG signals. Behavioral and Brain Functions 7, 30.

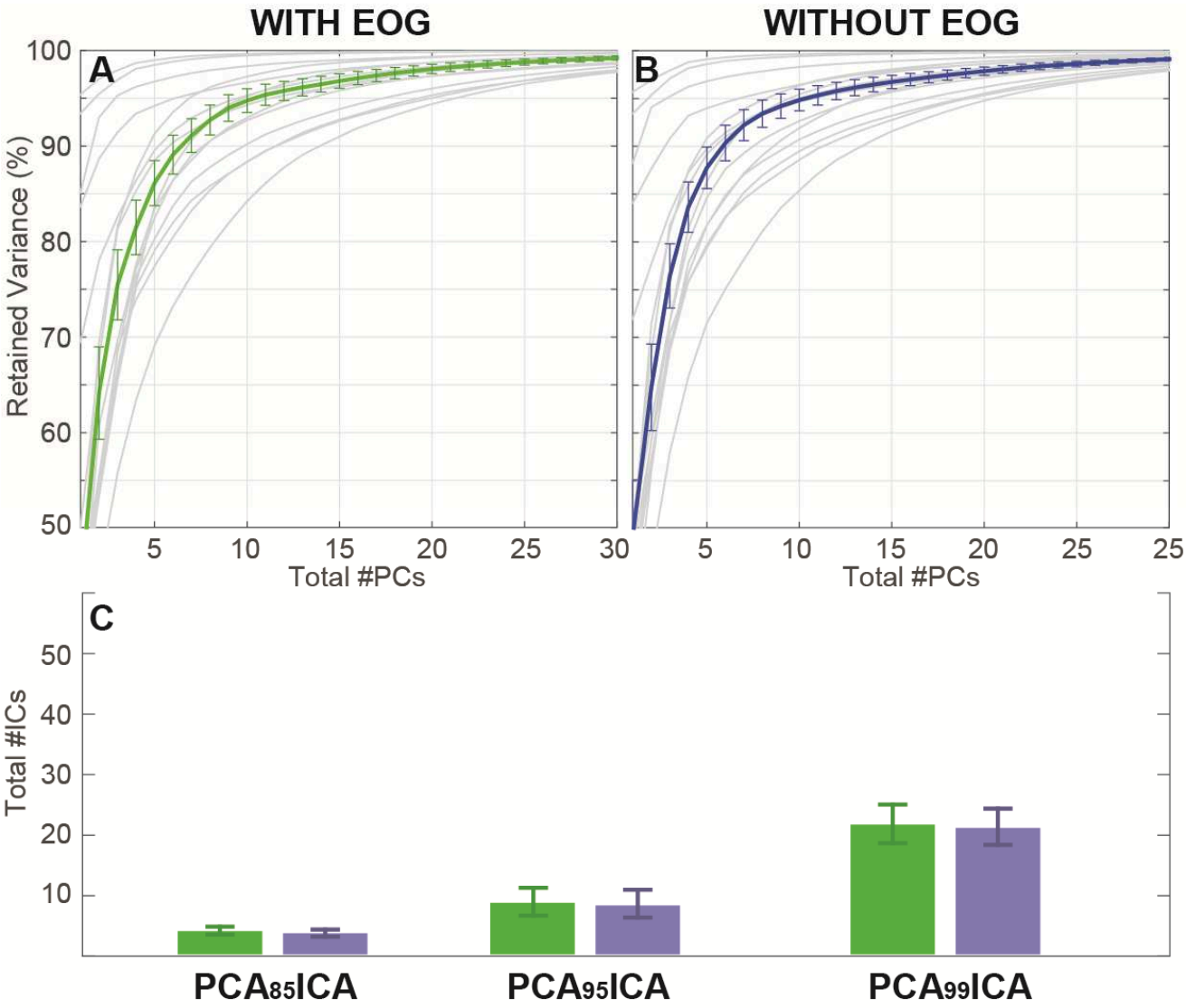

Figure 1: Mean explained variance (blue line) in relation to the number of largest principal components (PCs) retained, including (A) or not including (B) the bipolar vertical and horizontal electro-oculographic channels (EOGv and EOGh). Panel C shows the average number of PCs necessary to explain at least 85%, 95%, 99% of original dataset variance, including (green) or not including (blue) the EOG.

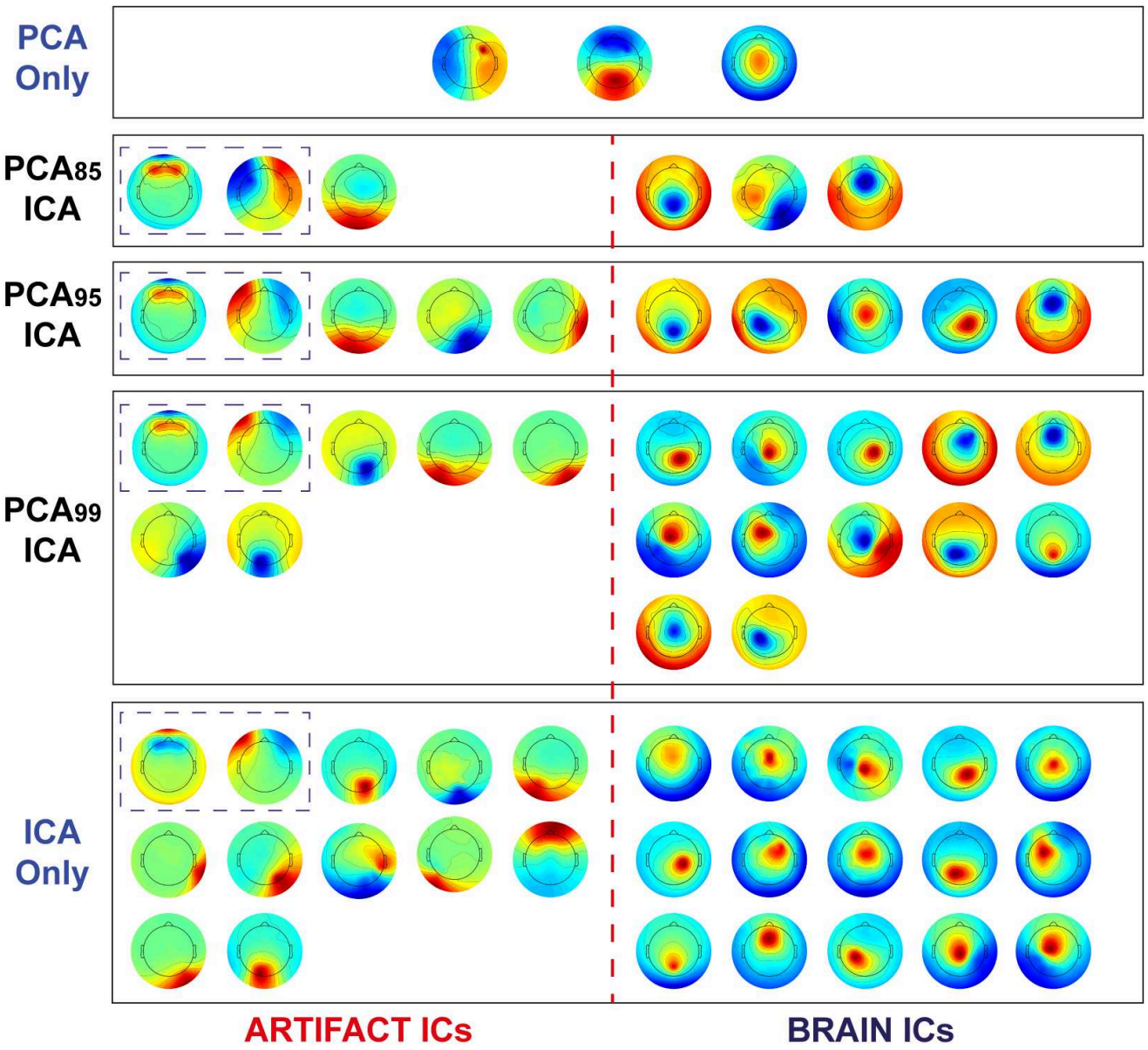

Figure 2: For a representative subject, scalp maps of quasi-dipolar components (dipolarity above 85%) extracted by applying ICA (ICA-Only) or PCA (PCA-Only) directly to the data, or by performing ICA after reducing the original data rank by PCA so as to retain at least 85% ($PCA_{85}ICA$, 4 ± 0.5 Median ± MAD PCs), 95% ($PCA_{95}ICA$, 8 ± 2.5 PCs) and 99% ($PCA_{99}ICA$, 21 ± 6 PCs) of data variance respectively. Components are sorted into identifiable non-brain Artifact and Brain ICs, separated by the vertical red dashed line. A dashed blue box highlights eye activity-related artifact ICs (vertical EOG and horizontal EOG ICs, respectively) in the $PCA_{95}ICA$, $PCA_{99}ICA$, and ICA-Only conditions.

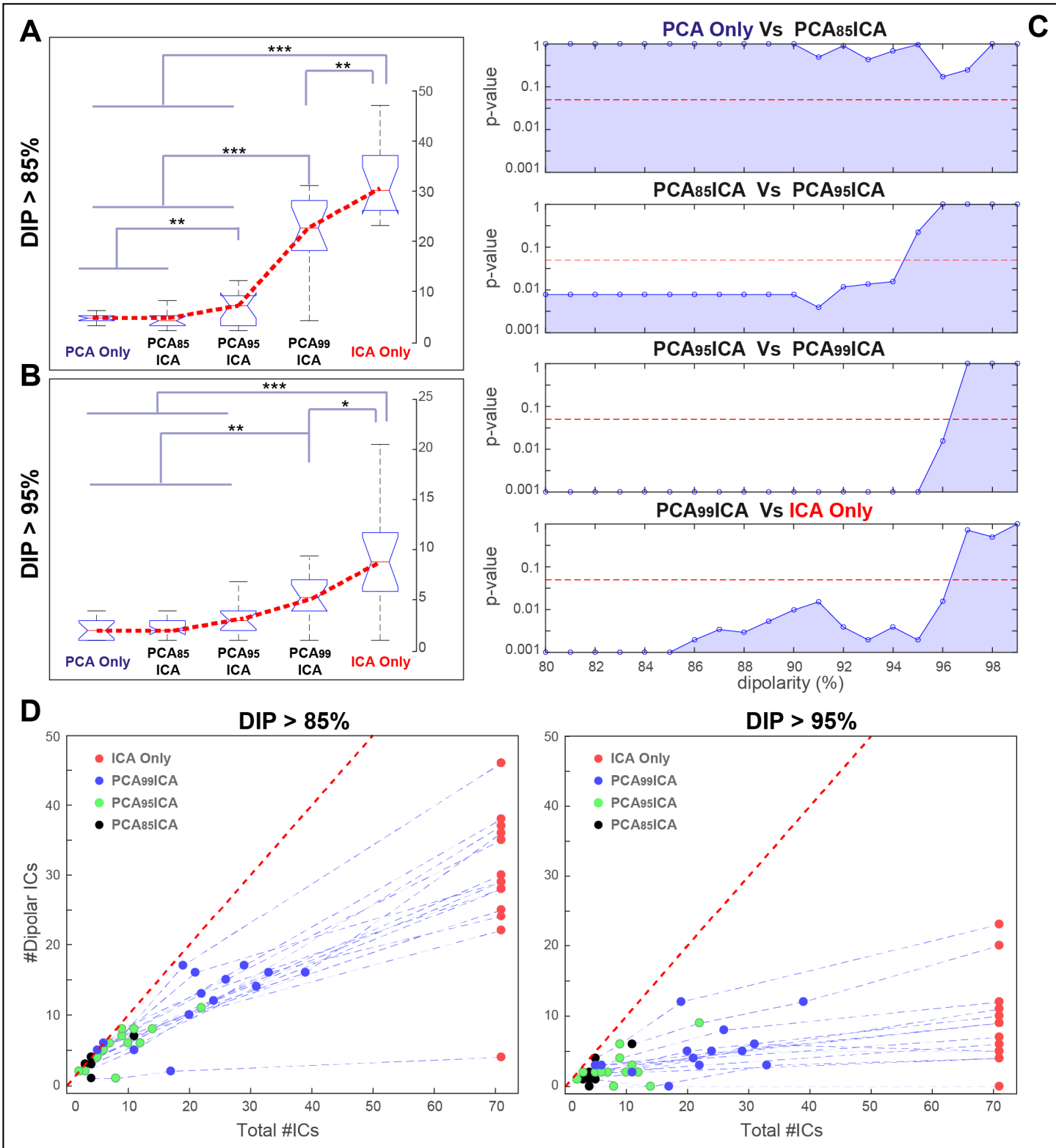

Figure 3: Panels A and B: box plots of median numbers of ICs (#ICs) with dipolarity values (A) above 85% (quasi-dipolar) and (B) 95% (near-dipolar). Significance of differences between conditions was determined using Kruskal-Wallis plus Tuckey *post hoc* tests. **Panel C**: Estimated probabilities of significant condition differences in the number of quasi-dipolar components (RV > 85%) for the following comparisons: (i) PCA-Only versus PCA$_{85}$ICA; (ii) PCA$_{85}$ICA versus PCA$_{95}$ICA; (iii) PCA$_{95}$ICA versus PCA$_{99}$ICA; (iv) PCA$_{99}$ICA versus ICA-Only. Each panel shows p-values for existence of significant differences between the number of quasi-dipolar components in the contrasted condition pair for each dipolarity threshold (x axis, RV > 80% to RV>99%). Dashed red lines show the dipolarity condition-difference significance threshold (red dashed line at p=0.05). **Panel D**: Numbers of dipolar ICs (y axis) available after PCA dimensionality reduction for two dipolarity thresholds (dipolarity > 85%, >95%) in decomposition conditions PCA$_{85}$ICA (black dots), PCA$_{95}$ICA (green dots), PCA$_{99}$ICA (blue dots), and ICA-only (red dots). A dashed blue line connects the dots for each subject. A red dashed line plots the #ICs (the upper bound to the #dipolar ICs).

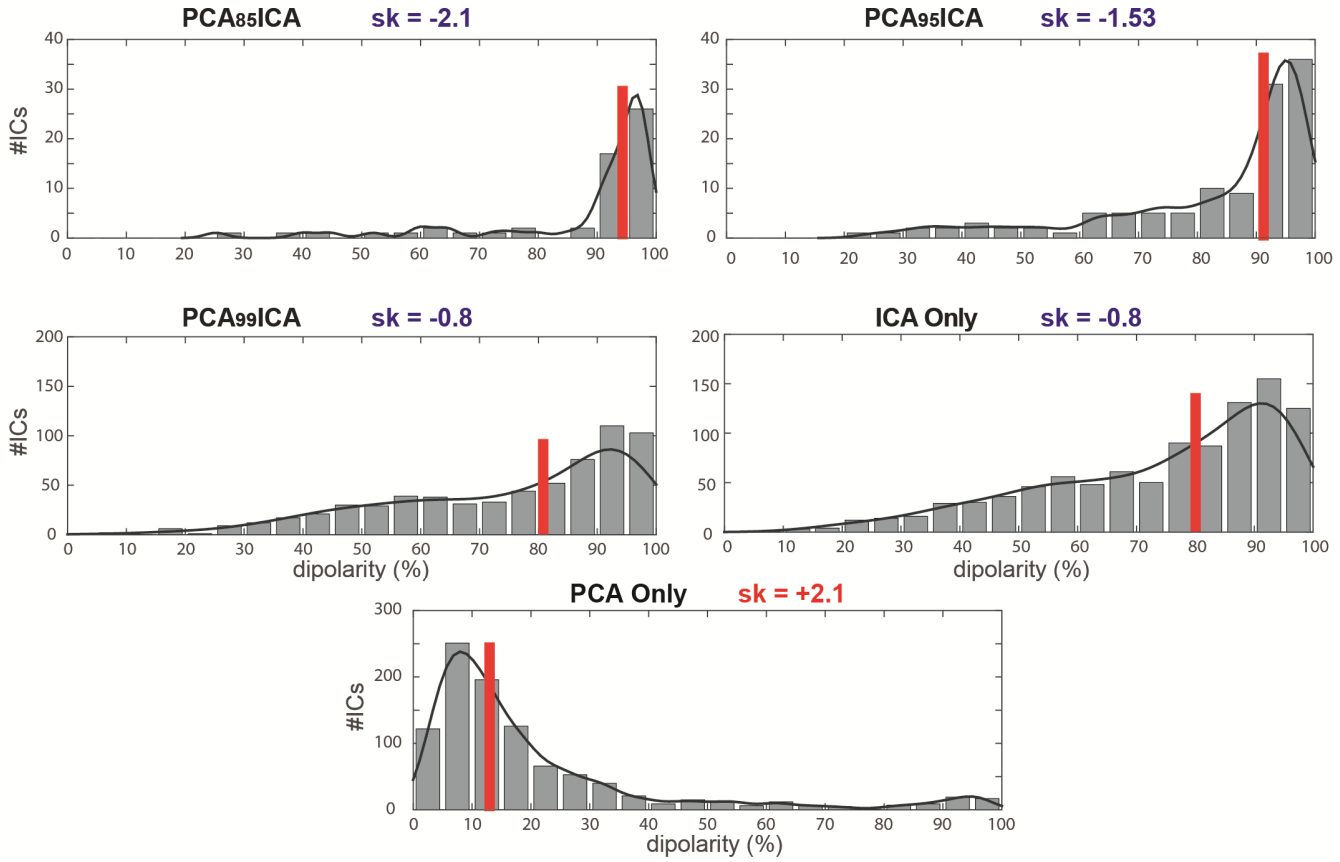

Figure 4: Histograms of component dipolarities (across all 14 data sets) following preliminary PCA subspace restriction (to RV>85%, RV>95%, or RV>99%), without preliminary PCA (ICA-Only), or directly applying PCA (PCA-Only). The median of each distribution is indicated by a red vertical line (sk = skewness). Note the different y-axis scales.

1

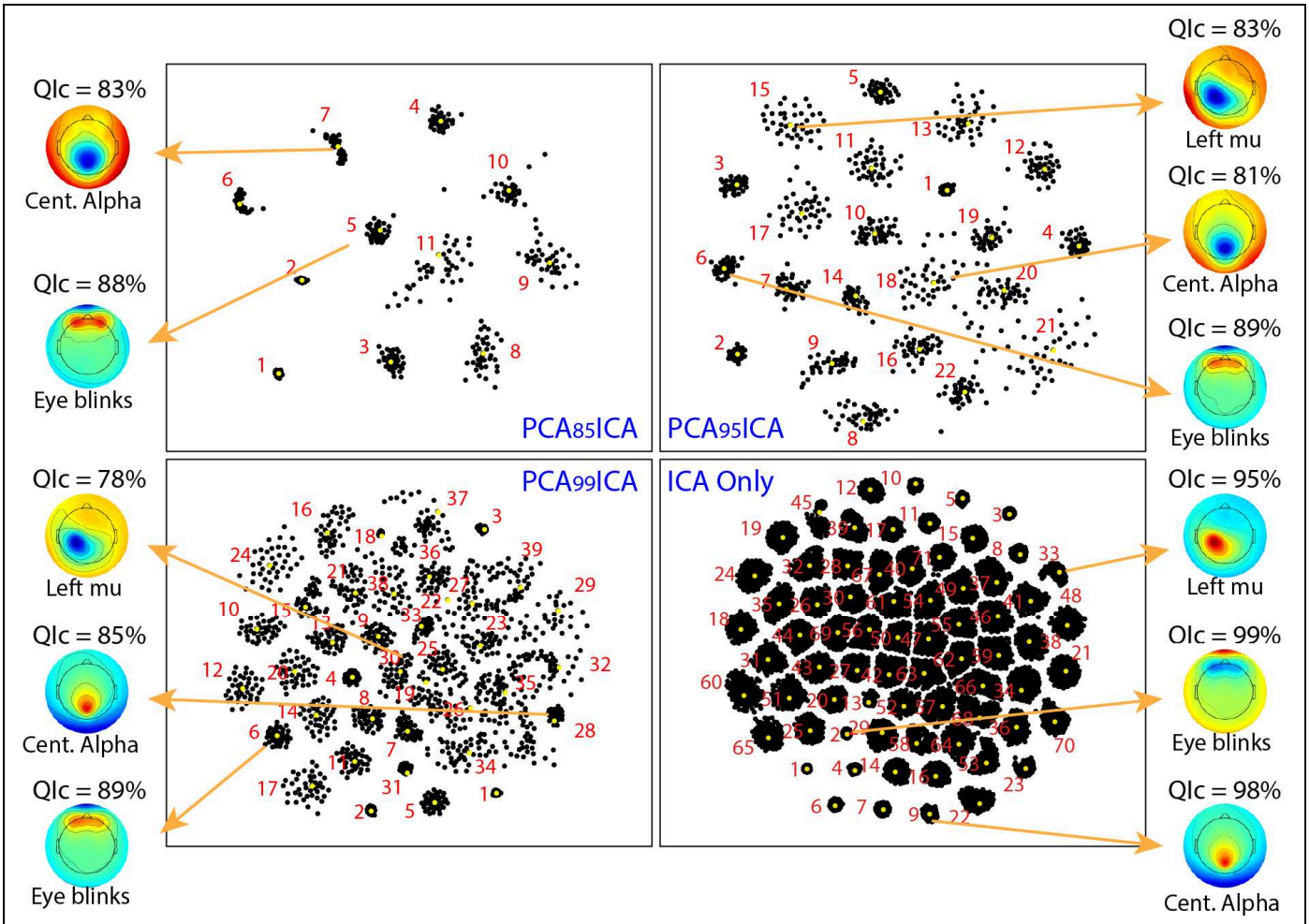

Figure 5: IC clusters extracted by RELICA bootstrap decompositions for one subject, either following reduction of data rank to a principal subspace ($PCA_{85}ICA$, $PCA_{95}ICA$ and $PCA_{99}ICA$) or (lower right) without PCA-based rank reduction. Within each box, the ICs are clustered according to mutual similarity and cluster quality index (QIc) values are computed to measure their compactness. At far left and right, scalp maps of example components in clusters associated with left hand-area (8-12 Hz) mu rhythm activity, central posterior (8-12 Hz) alpha band activity, and eye blink artifact are shown and their QIc values are indicated. Note the stronger between-subject cluster definition and higher QIc values (reflecting more highly correlated time course) for the IC clusters without PCA processing (ICA-Only, lower right).

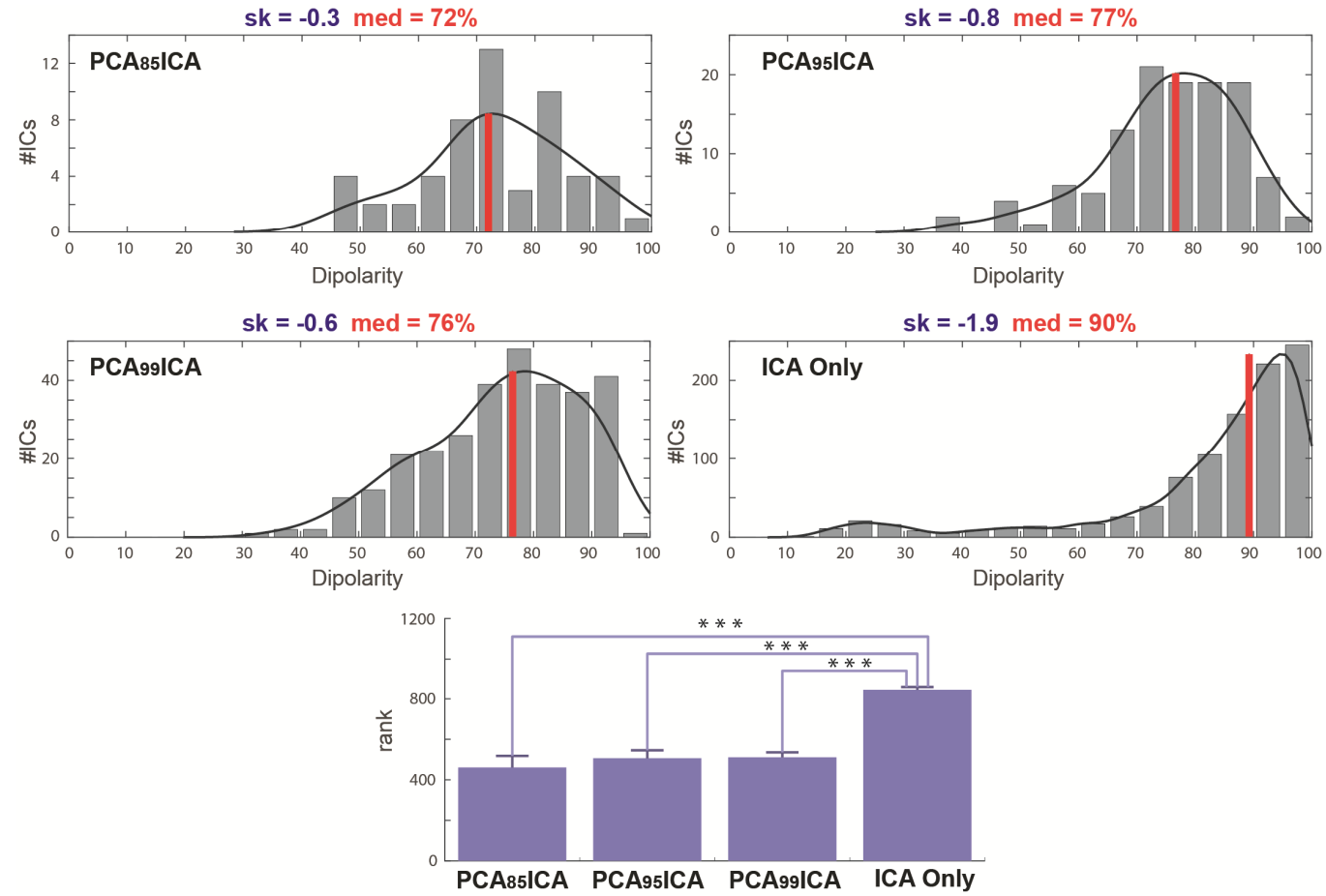

Figure 6: Distribution of IC QIc values across the subjects for different levels of principal subspace data variance retained ($PCA_{85}ICA$, $PCA_{95}ICA$, $PCA_{99}ICA$) and for ICA-Only (100%). The median of each distribution is indicated by a red vertical line (med = median; sk = skewness). **Bottom panel:** Significance of pairwise differences between conditions, determined using a Kruskal-Wallis test with Tuckey post hoc correction for multiple comparisons correction (*** = p<.001).

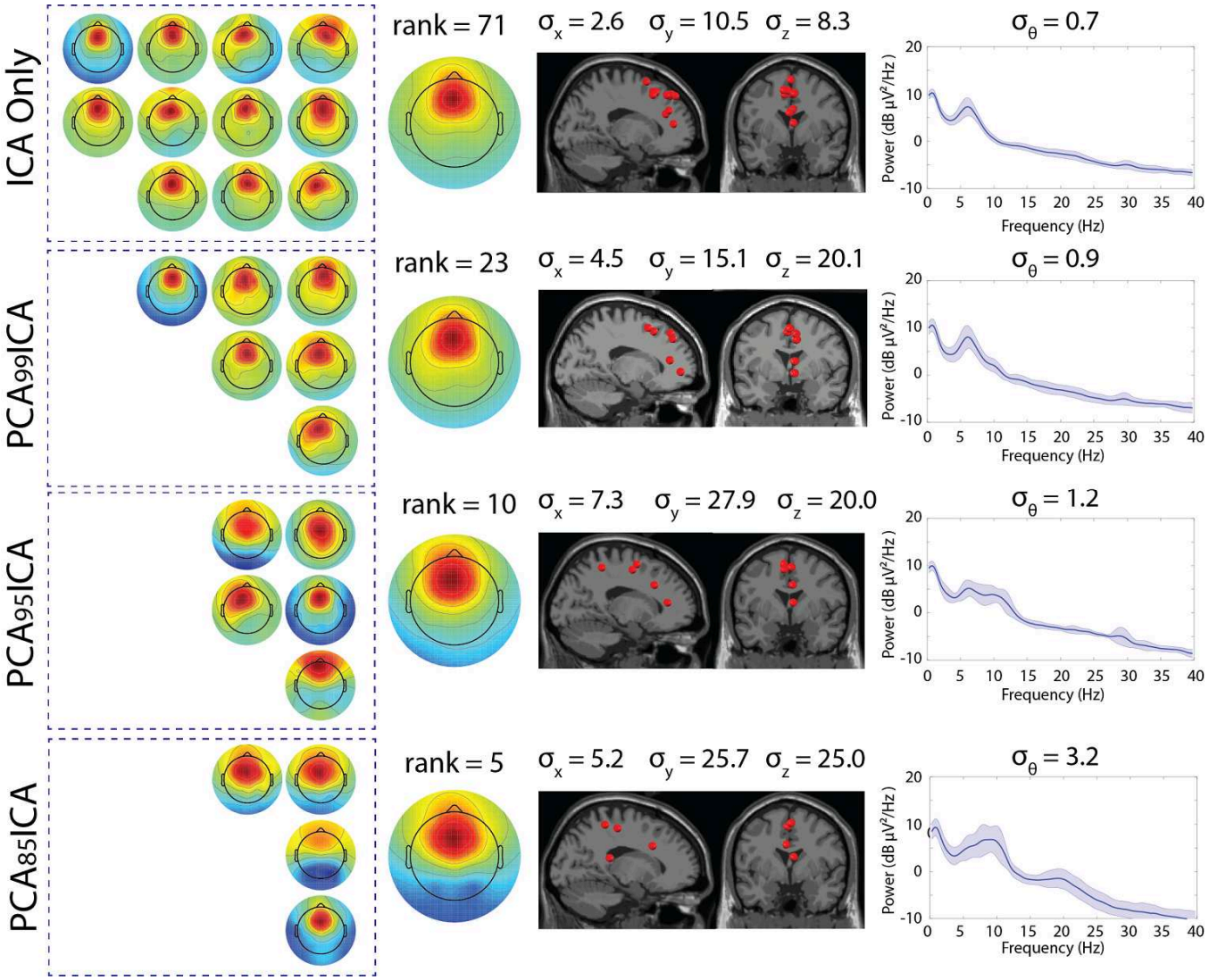

Figure 7: The frontal midline theta (fMθ) cluster identified across subjects in each of the four decomposition conditions ($PCA_{85}ICA$, $PCA_{95}ICA$, $PCA_{99}ICA$ and ICA-Only) conditions. The picture shows the individual IC scalp maps (1st column), the cluster-mean maps (2nd column), IC equivalent dipole locations (3rd column – each dot represents one IC for one subject). The median absolute deviations (MAD; $\sigma_x, \sigma_y, \sigma_z$ in mm) of the cluster IC equivalent dipole positions are given. The 4th column shows cluster median power spectral densities (PSDs, with ± MAD shaded). σ_θ, the MAD of the PSD in the (4-8 Hz) theta band is also indicated.

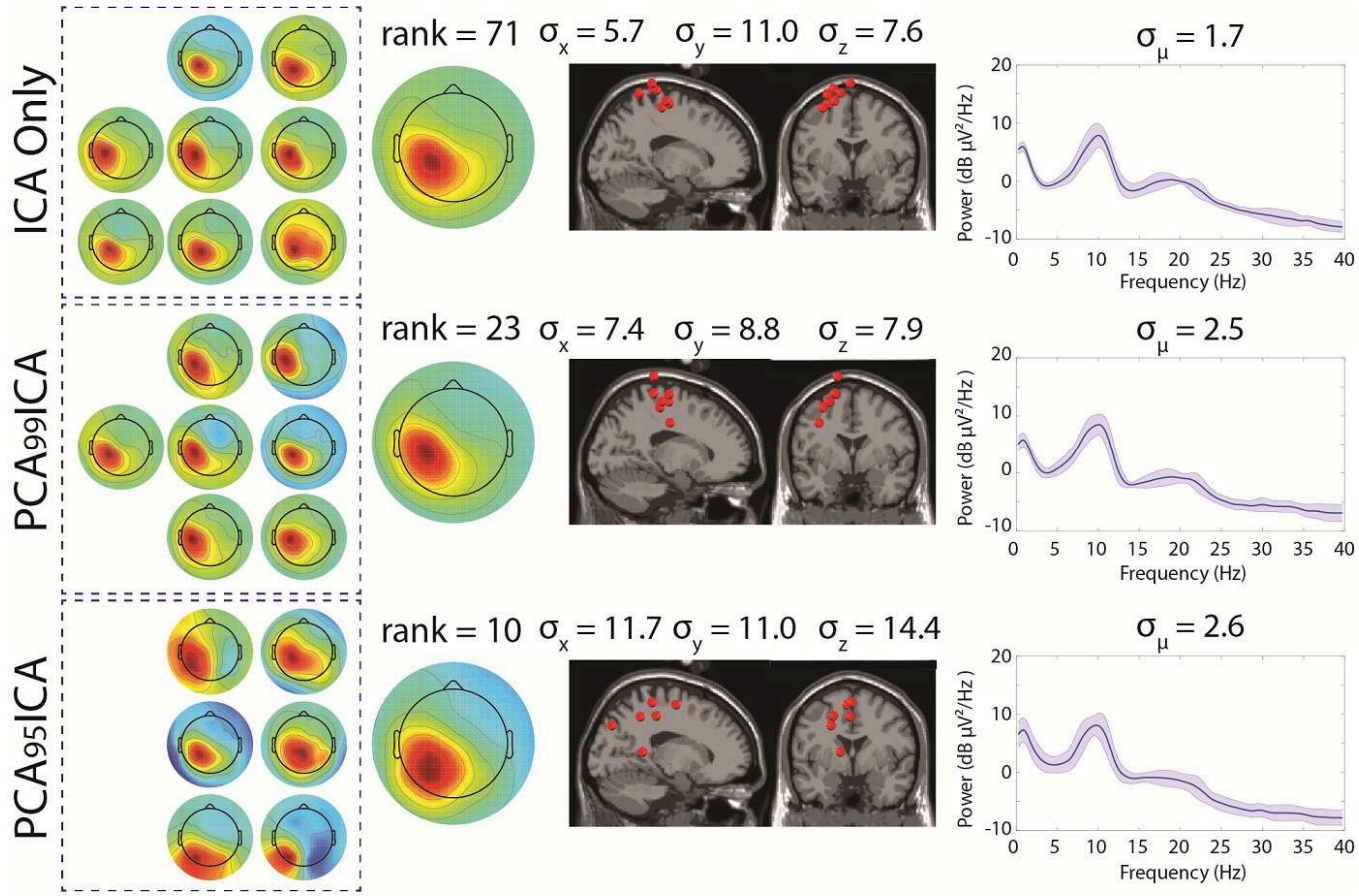

Figure 8: Left mu clusters across all subjects for the $PCA_{85}ICA$, $PCA_{95}ICA$, $PCA_{99}ICA$ and ICA-Only decomposition pipelines. The picture shows the individual IC scalp maps (1st column), cluster mean scalp map (2nd column), IC equivalent dipole locations (3rd column – each dot represents an IC of one subject), and in the 4th column, the cluster median (± 9-11 Hz MAD) PSD. This is another example of the effects of PCA dimension reduction at the across-subjects cluster level (cf. Figure 7).